Theoretical Investigation of Hydrogen Desorption Process in Hydrogen Boride sheet for Catalytic Applications

Kurt Irvin M. Rojas[1], Yoshitada Morikawa[1,2], and Ikutaro Hamada[1]
[1]Department of Precision Engineering, Graduate School of Engineering, Osaka University
[2]Research Center for Precision Engineering, Graduate School of Engineering, Osaka University

1. INTRODUCTION

New classes of 2D materials are the subject of recent research efforts for a variety of applications (e.g. electronics, energy storage, catalyst). The high surface density of these 2D materials makes them ideal for H_2 storage and catalysis. In particular, the newly synthesized hydrogen boride (HB) sheets are a promising material for H_2 storage due to their inherent high hydrogen composition. This HB sheet can be reliably synthesized from MgB_2 with a yield of 42%.[1]

Recent studies have shown that H_2 extraction is possible by using heat treatment or photon irradiation which can extract about 94% of the total hydrogen composition.[2] The noteworthy storage and extraction yield is a significant advantage over bulk metals and alloy based H_2 storages. We also found in our previous study that it is remarkably stable against water,[3] a common substance in ambient condition and fuel cell technologies, making HB sheets a promising material for hydrogen storage applications. To further investigate its viability, there is a need to study the cyclic hydrogen discharge-recharge process. In particular, the effect on the stability and structure of hydrogen deficiency is unclear.

In addition, HB sheets have been shown to be a promising catalyst for ethanol reforming and carbon dioxide conversion.[4] However, in the experimental process, the HB sheets are subjected to heat pre-treatment that induces hydrogen desorption and releases about 33-50% of the hydrogen composition, meaning the experimental condition of the HB sheets are in a hydrogen deficient state.

In both hydrogen storage and catalyst applications, the condition of the hydrogen deficient HB sheet is important to understand. For simulation studies, to effectively study the reaction processes, an accurate representation of the hydrogen deficient HB sheet structure is required.

In this study, we investigate the structure of the hydrogen deficient HB sheet at varying levels of hydrogen vacancy saturations using a workflow involving machine learning assisted structure search with a density functional based tight binding (DFTB) method as a target potential. This is followed up by accurate optimization using the density functional theory (DFT) method. Finally, we obtain a set of the most energetically favored structures with varying hydrogen content.

2. METHODOLOGY

In the pursuit of exploring novel structures, particularly in complex scenarios like high-dimensional structure searches where local optimization falls short, the demand for a robust and efficient global optimization (GO) algorithm is imperative. This study employs GOFEE (global optimization with first-principles energy expression) algorithm, integrated within the AGOX package,[5] as the GO algorithm of choice. Conventional GO

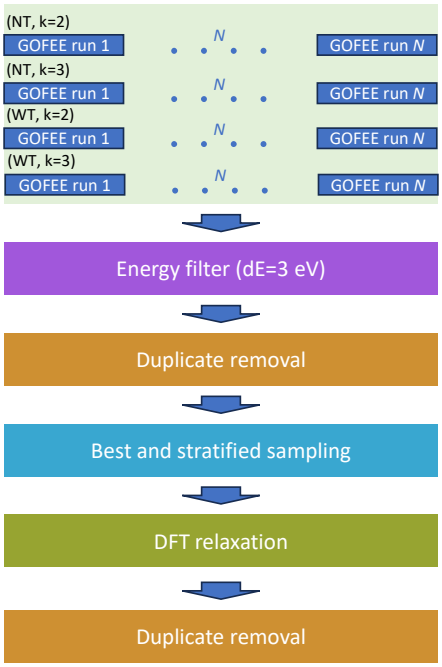

Figure 1. Workflow diagram.

methods typically entail resource-intensive computations for energy and force evaluations, compounded by entirely random structure propagation, diminishing the likelihood of converging to the global minimum (GM). GOFEE introduces two pivotal innovations. First, it mitigates computational burdens by employing a Gaussian process regression (GPR) model, iteratively train on-the-fly using the target potential – here, Density Functional Tight Binding (DFTB) method as implemented in the DFTB+ package [6] – to handle energy and force evaluations during local optimization steps. Secondly, rather than relying on random structure propagation, a genetic algorithm is adopted. This approach entails generating subsequent structures for evaluation by iteratively applying mutations to preceding structures.

In the following discussion, we explain the workflow of the structure search as described in Fig. 1. The first step is initializing four sets comprising 30 independent instances of GOFEE calculations. This entails seeding each calculation differently, making the initial state of the search distinct from each other. For a more comprehensive search, we included two variations of GOFEE calculation: template and κ

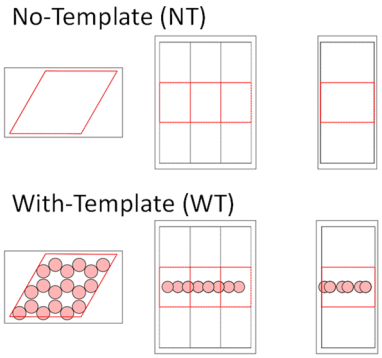

Figure 2. Graphical model of the with-template and no-template initial state.

parameter. In the template variation, we considered two starting structures, a no-template (NT) and a with-template (WT) setup (refer to Fig. 3). The NT configuration allows GOFEE complete freedom to place all hydrogen and boron atoms while the WT initializes with a 2D boron sheet that creates a bias towards a sheet-like structure and only allows GOFEE to place the hydrogen component. The κ governs the exploratory-exploitative tendency of the search and was varied to values of 2 and 3. The lower κ value nudges the balance towards a more exploitative direction. The combination of these two variations results in four sets of GOFEE calculations that are distinctly initialized. The mutations applied are random and rattle mutations with a 6:14 ratio in the 20 samples. A dual-point evaluation was also performed with the second point a small nudge towards the force direction. With 500 iterations, a cumulative total of 120,000 structures are evaluated, resulting in the identification of the GM structure and its corresponding energy.

Subsequently, the second step involves a reduction in the number of structures by eliminating those exceeding 3eV from the GM energy. Following this, the third step entails duplicate removal. Here, we employ a group strategy for atomic structures utilizing the eigenvalues of the distance-based Laplacian matrix, implemented within AGOX. This comparison method exhibits insensitivity to minor fluctuations in bond

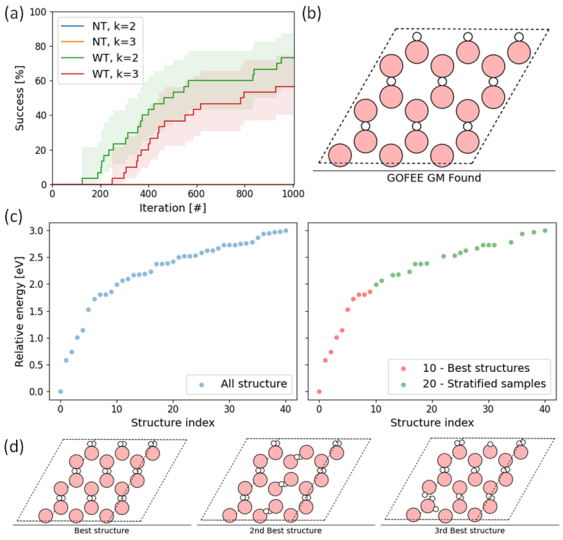

Figure 3. Workflow results on pristine HB sheet. (a) shows the success rate on finding and converging to a global minimum shown in (b). In (c), a graphical representation of the sampling strategy is shown. Lastly, (d) shows the 3 best DFT-optimized structures.

lengths, thereby effectively clustering structures with similar eigenvalues. Within each group, we opt for the energetically most favorable structure. In the fourth step, a further reduction in the number of structures is achieved through a simple sampling technique. Specifically, we select the 10 lowest energy structures and choose 20 structures by stratified sampling from the remaining unselected structures, resulting in a total of 30 structures.

Continuing with the fifth step, we proceed to further optimize all 30 structures until the forces are below 10^{-4} Ry/Bohr. This optimization is conducted using DFT, implemented within the Quantum Espresso package.[7] Herein, a k-point mesh of 6x6x1 is employed, alongside a tight self-consistency threshold of 10^{-9}, and wavefunction (charge) cutoff energy of 60 (480). The exchange-correlation functional was approximated using rev-vdW-DF2 to effectively account for the vdW interactions.[8] The pseudopotentials generated using the Perdew-Burke-Ernzerhof formulation of the generalized gradient approximation were adopted from the GBRV ultrasoft pseudopotential library.[9] Finally, the duplicate removal step is reapplied to yield the final set of structures, wherein the true GM manifests as the most energetically favored configurations within the set.

3. RESULTS AND DISCUSSION

3.1 PRISTINE HB SHEET

As a preliminary benchmark, we initially subject a pristine HB sheet to the workflow. Figure 3 provides a summary of the results obtained from the workflow steps. Notably, in terms of success rates (Fig. 3a) converging on the GOFEE GM structure (Fig. 3b), the WT approach demonstrates a high success rate of approx. 70%. Conversely, the NT approach encounters challenges in locating the GM, likely due ot the increased complexity inherent in the initial unbaised state, necessitating more iterations copared to the WT approach. Figure 3c illustrates the graphical representation of the sampling strategy, which entails selecting the top 10 structures along with the 20 stratified structure samples. Subsequently, all 30 structures undergo optimization using the DFT method, and the top three structures showcased in Figure 3d. It is noteworthy that the optimal structure post-optimization is identical with the GM identified in the preceding GOFEE calculation.

3.2 HYDROGEN-DEFICIENT HB SHEET

To emulate the experimental condition, a few models corresponding to 11, 22, 33, and 44 at% hydrogen deficiencies were used. The summary of the structure search findings is presented in Figure 4. In all cases the GOFEE calculation successfully obtained the GM within the iteration span. Interestingly, the higher hydrogen deficiency (e.g. 44 at%) converges much faster compared to lower hydrogen deficiency. The GMs found by deficiency 22 at% and greater show a more complex configuration of the bridge hydrogen. It seems the desorption process does not simply remove

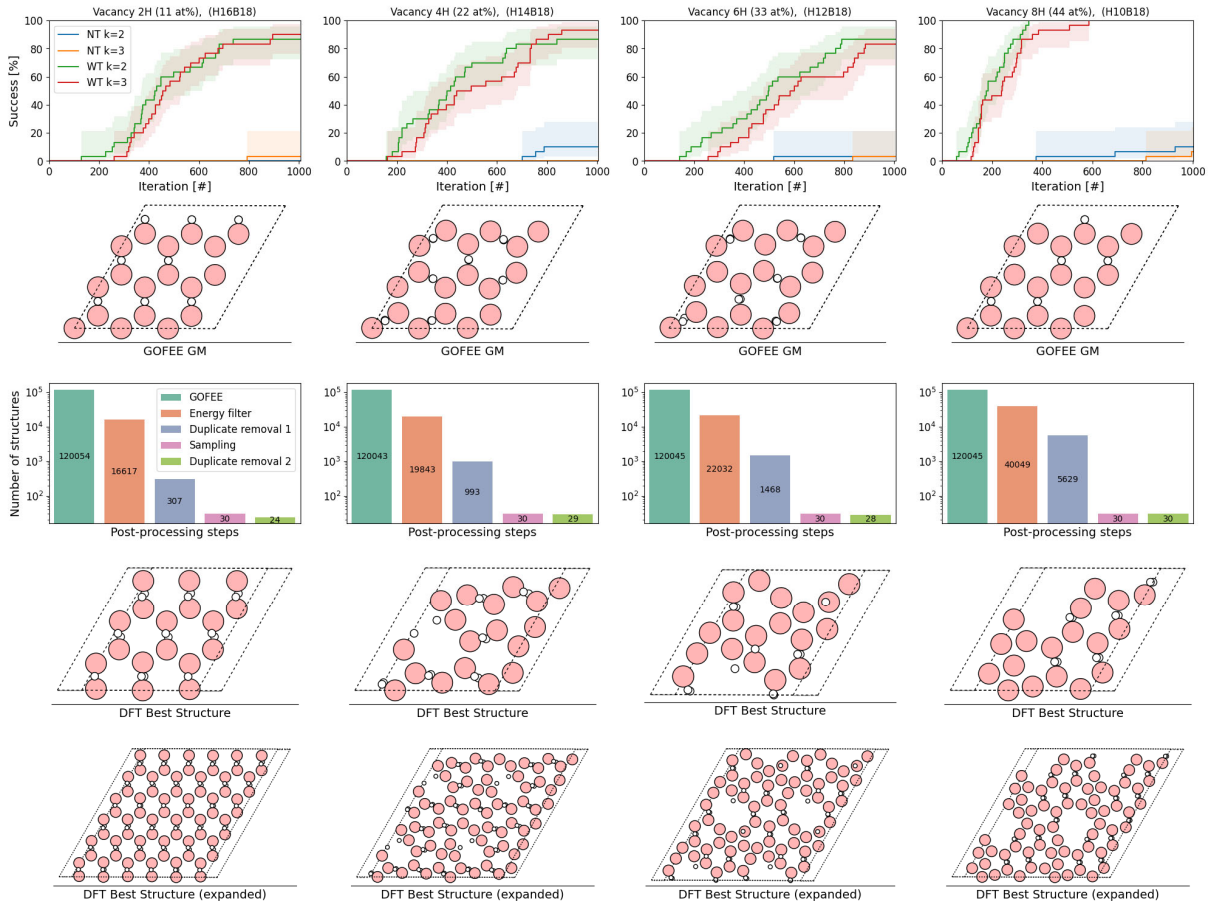

Figure 4. Summary of the structure search workflow on hydrogen-deficient HB sheet at varying level of deficiency.

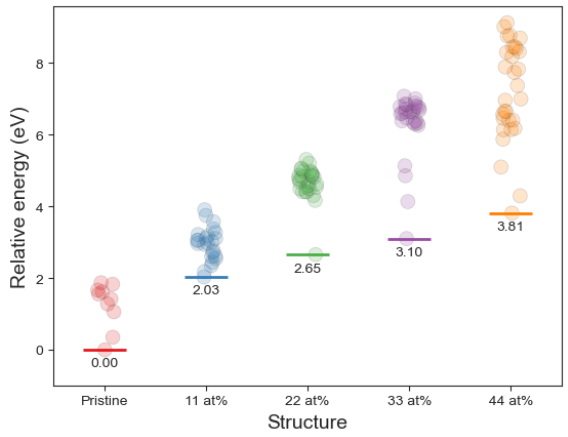

Figure 5. Relative energy of the hydrogen deficient structures.

the hydrogen atoms but instead also induces reconfiguration on the remaining hydrogen atoms. In the post-processing steps, duplicate removal on 11 at% deficiency has significant effects but as the deficiency increases, the impact reduces due to the increasing complexity of the system. This complexity stems from the lack of enough atoms to form a periodic and symmetric structure making a tendency to form more "chaotic" structures. This is also why the NT has increased rates at high deficiency – because the GM found by WT was more chaos and close to NT performance. The best DFT structure are also presented. In all cases, the best structure is not identical to the GOFEE GM found, meaning that the final DFT optimization is a better and more accurate approach in obtaining true GM. Lastly, the best DFT structure was artificially expanded along its periodic direction for a clearer visualization of the holes created in the desorption process.

Finally, we describe the relative energies of the discovered structures. In all deficient cases, the relative energy shows that the structure is less stable than the pristine structure. Interestingly, the largest energy step increase is in the step from pristine to 11 at%. The succeeding increase in deficiency saturation

did further destabilize the structure but not to the same magnitude as the first step. This means that the desorption process bottleneck happens in the initial hydrogen desorption step, and succeeding hydrogen desorption will be easier. Additional calculations on energy barriers are still required to further investigate this aspect.

4. CONCLUSION

In conclusion, our study explores the structure and stability of hydrogen deficient HB sheets. Leveraging a machine-learning-assisted structure search workflow, we elucidate the effect of varying levels of hydrogen deficiency on the structural configuration and stability of HB sheets.

The structure at varying levels of hydrogen deficiency is described in detail. These set of structures can be a baseline model for future calculations that needs a more accurate HB sheet environment in high temperature conditions. As observed, the increase in hydrogen deficiency also increasingly destabilizes the structure. The largest destabilization happens at the first step – from pristine to 11 at% deficiency.

REFERNCES

(1) Nishino, H. et al., J. Am. Chem. Soc. 139, 13761–13769 (2017).

(2) Kawamura, R. et al., Nat. Commun. 10, 4880 (2019).

(3) Rojas, K. I. M. et al., Commun. Mater. 2, 81 (2021).

(4) Goto, T. et al., Commun. Chem. 5, (2022).

(5) Christiansen, M. P. V., et al., J. Chem. Phys. 157, (2022).

(6) Hourahine, B. et al., J. Chem. Phys. 152, (2020).

(7) Giannozzi, P. et al., J. Phys. Condens. Matter 21, 395502 (2009).

(8) Hamada, I., Phys. Rev. B - Condens. Matter Mater. Phys. 89, 121103 (2014).

(9) Garrity, K. F., et al., Comput. Mater. Sci. 81, 446–452 (2014).